2011

Swarm Control Through Symmetry and Distribution Characterization

Georgi Dinolov
Harvey Mudd College

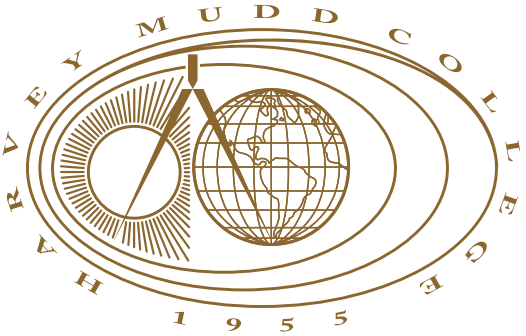

Swarm Control Through Symmetry and Distribution Characterization

Georgi Dinolov

Rachel Levy, Advisor

Dagan Karp, Reader

May, 2011

HARVEY MUDD
COLLEGE
Department of Mathematics

Abstract

Two methods for control of swarms are described. The first of these methods, the Virtual Attractive-Repulsive (VARP) method, is based on potentials defined between swarm elements. The second control method, or the abstraction method, is based on controlling the macroscopic characteristics of a swarm. The derivation of a new control law based on the second method is described. Numerical simulation and analytical interpretation of the result is also presented.

Acknowledgments

Special thanks go out to Professors Rachel Levy, Nick Pippenger, Dagan Karp, and Andrea Bertozzi (UCLA) for spending time with me to discuss the topics covered in this work.

Contents

List of Figures

Chapter 1

Introduction

In nature, large collections of individuals, usually from the same species, cluster together and behave as a single entity. These entities are commonly referred to as *swarms*. Types of swarms that may immediately come to mind are a school of fish or a locust swarm, illustrated in Figure 1.1. Attempts have been made to model the behavior of swarms by reproducing behavior observed in biology. Such behavior can be classified in two ways

1. Perceived coordination between individuals (microscopic scale);
2. A unified goal/action of the swarm (macroscopic scale).

In the school of fish of Figure 1.1a, we may characterize the coordination between individuals as maintaining a maximum distance between neighbors and a minimum speed, and the unified goal/action of the swarm may be identified as moving in a coordinated, clockwise circular formation. Similarly, for the locusts, the microscopic behavior could be characterized as maintaining a maximum distance between neighbors while the perceived

a. Fish swarm

b. Locusts swarm

Figure 1.1 Depicted are swarms in nature.

behavior on the macroscopic scale could be the swarm having a constant volume defined by the boundaries of the group.

1.1 Motivation

The two characteristics of swarm behavior may be viewed as two sides of the same coin. Interactions between individuals give rise to perceived macroscopic behavior, and the unified goal of a swarm is what defines behavior between individuals. Biologically, the question of which characteristic is dominant could be a very complicated one, and it is far beyond the scope of this work. However, in terms of analysis and application, both views are equally valuable and will be discussed in the following chapters.

Engineers and mathematicians are interested in modeling swarms because such systems have particularly useful applications. Often, complex and time-consuming tasks can be accomplished much more efficiently by a coordinated collection of individuals than by extensive efforts of a singleton. For example, in searching for a target in the open ocean, a group of drones could find the object faster if they share information about where they have been and what they have observed than if they worked independently. In their work, Kurabayashi et al. (2002) utilize the concept of cooperation in devising a coordination algorithm for a group of robots for effectively sweeping a given work area. The examples of drones and robots working together to accomplish a task illustrate the central importance of swarm behavior to applied problems. Swarms are valuable as general structures because the *collective* capabilities of the group transcend those of the individuals comprising the group. However, as coordinated tasks become more complex, it is first necessary to understand how to *control* a swarm. It is the goal of this work to explore and develop mathematical methods for such control.

1.2 Direction

Chapter 2 introduces the Virtual Attractive-Repulsive Potential method for controlling swarms by imposing specific intraparticle interaction laws. Chapter 3 introduces a "macroscopic-first" approach as outlined by Belta and Kumar (2004) that derives the controls for the members of a swarm by first defining macroscopic behaviors. Chapter 4 describes the derivation of a new control law based on the "macroscopic-first" approach aiming to create a uniform disk distribution on a swarm; Section 4.6 goes through the

numerical simulation results and analytical interpretation of the results. Chapter 5 concludes with future work direction.

Chapter 2

The Virtual Attractive-Repulsive Potential Method

The "Virtual Attractive-Repulsive Potential Method" (VARP from hereon) is a general control approach used by Nguyen et al. (2005). Simply put, this method imposes a virtual potential function on each member of the swarm, whose gradient is the potential force vector establishing the controls for the member of the swarm. In this chapter, the basic idea behind the model is given in Section 2.1. The model is then developed in Sections 2.2 and 2.3, with Equation 2.4 being the control law due to the VARP method.

2.1 Model Basics

In the VARP method we seek to guide a group of individuals (the swarm) from a starting position to a final destination. Along the way, the swarm should avoid collisions between individuals and collisions of individuals with obstacles.

Two types of environmental objects have potentials associated with them. Targets are attractors (having a negative potential), while obstacles are repulsors (having a positive potential). Swarm elements have both positive and negative components of their potentials. The reason for this duality in that we want the elements to stay together but also avoid colliding.

2.2 The Virtual Attractive-Repulsive Potential

The potential function $V(z)$ which generates virtual force vectors guiding the swarm can take many forms, but its defining quality is that its argument is a scalar representing distance. Given an i^{th} element in the swarm, the potential for that element is

$$V_i = \sum_k V_{\text{attractors}}\left(||\Delta\vec{z}_{i,k}||\right) + \sum_l V_{\text{repulsors}}\left(||\Delta\vec{z}_{i,l}||\right) + \sum_{j(j\neq i)} \left[V_a\left(\left|\left|\Delta\vec{z}_{i,j}\right|\right|\right) + V_r\left(\left|\left|\Delta\vec{z}_{i,j}\right|\right|\right)\right]. \tag{2.1}$$

$V_{\text{attractors}}$ gives the potential that an element feels due to an attractor, the index k ranges over all attractors in the environment, $V_{\text{repulsors}}$ gives the potential that an element feels due to repellers, and the index l ranges over all repellers in the environment. V_a, V_r are the attractive and repulsive components of the potential that element i experiences due to the j^{th} element, and the j index spans all elements in the swarm plus the repellers and attractors. $\Delta\vec{z}_{i,j}$ is a vector pointing from position of element i to position of element j, and $||\vec{v}||$ is the Euclidean norm in R^n, so that $\left|\left|\Delta\vec{z}_{i,j}\right|\right|$ is the distance between elements i and j. We will combine the attractive and repulsive parts of the potential function so that

$$V_i = \sum_{j(j\neq i)} \left[V_{\text{a}}\left(\left|\left|\Delta\vec{z}_{i,j}\right|\right|\right) + V_{\text{r}}\left(\left|\left|\Delta\vec{z}_{i,j}\right|\right|\right)\right]. \tag{2.2}$$

Note that repulsors can be environmental objects, and they are accounted for here as stationary elements.

The Potential Force Vector

The potential V_i for the i^{th} element in the swarm naturally creates a corresponding potential force vector, which is the gradient of the function. Namely, $F_i = \nabla V_i$, which, after the application of the chain rule, takes on the form

$$F_i = \sum_{j(j\neq i)} V'_{\text{a}}\left(\left|\left|\Delta\vec{z}_{i,j}\right|\right|\right) \frac{\Delta\vec{z}_{i,j}}{\left|\left|\Delta\vec{z}_{i,j}\right|\right|} + V'_{\text{r}}\left(\left|\left|\Delta\vec{z}_{i,j}\right|\right|\right) \frac{\Delta\vec{z}_{i,j}}{\left|\left|\Delta\vec{z}_{i,j}\right|\right|}. \tag{2.3}$$

The above force F_i is the control for each element in the swarm. Nguyen et al. (2005) used this control model on a collection of propeller-driven robots. To implement the model, the *virtual* force F_i was equated to the force

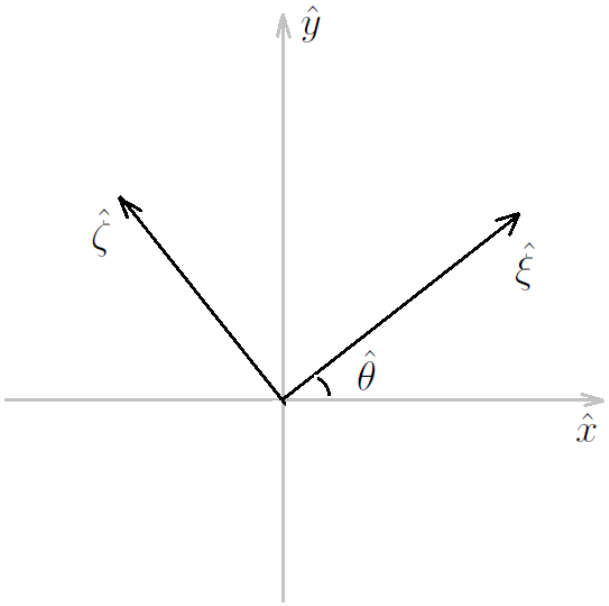

Figure 2.1 The Lagrangian frame, represented by the $\xi\zeta$-axis, is offset by θ from the Eulerian frame, represented by the xy-axis. The figure was obtained from Nguyen et al. (2005).

generated by each robot, thereby causing the robots to behave according to the model. The process of equating the virtual force to that generated by each robot is given in Section 2.3.

2.3 Force Balancing

The model proposed by Nguyen et al. (2005) equates Equation 2.3 to the forces generated by robots used for experimentation, with a small modification. To properly describe this modification, let $\vec{z}_i$ be the location of the i^{th} element, $\vec{w}_i$ its velocity, and m its mass. Furthermore, we define a Lagrangian, right-hand oriented coordinate system $\xi\zeta$ (Figure 2.1), where an angle θ denotes the offset of the ζ-axis from the x-axis in the Eulerian frame.

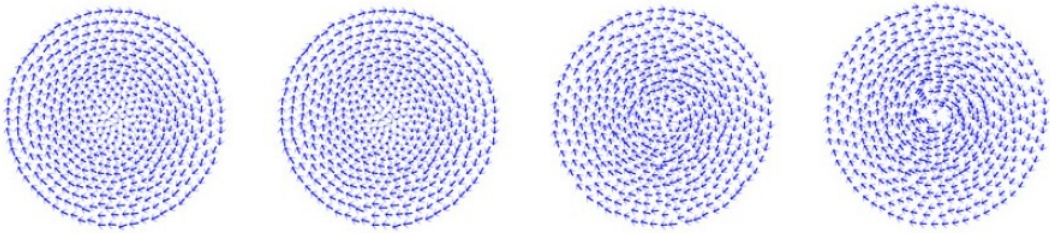

Figure 2.2 Depicted is the effect of increasing the self-propulsion α term of the balance law in Equation 2.5. From left to right, the values for α in the graphs are 0.003, 0.03, 0.1, and 0.5. The swarm changes from rotating as a rigid body to rotating as a ring,; that is, a rigid body with a center area unoccupied by swarm members. The figure was obtained from Chuang et al. (2007).

Then

$$\begin{aligned} \frac{d\vec{z}_i}{dt} &= \vec{w}_i \\ m\frac{d\vec{w}_i}{dt} &= \alpha\hat{\xi}_i - \beta\vec{w}_i \\ &\quad + \sum_{j(j\neq i)} \left[V_{\mathrm{a}}'\left(||\Delta\vec{z}_{i,j}||\right) \frac{\Delta\vec{z}_{i,j}}{\nabla\Delta\vec{z}_{i,j}} + V_{\mathrm{r}}'\left(||\Delta\vec{z}_{i,j}||\right) \frac{\Delta\vec{z}_{i,j}}{\nabla\Delta\vec{z}_{i,j}} \right]. \end{aligned} \quad (2.4)$$

The additional term α is a magnitude for a self-propulsion force. By adding such a term, Nguyen et al. (2005) take into account that the robots always generate some constant force in the $\hat{\xi}$ direction and that the force due to the potential is added to it; β is a coefficient which takes into account the frictional forces experienced by the robots. The behaviors of systems with interaction forces such as those in Equation 2.4 are discussed by D'Orsogna et al. (2006) and Chuang et al. (2007). Changing the parameters of the intraswarm interactions alters the macroscopic behavior of the swarm, as might be expected. For example, Chuang et al. (2007) present the results of varying α in magnitude from 0.003 to 0.5 for a swarm composed of 500 individuals. In proceeding from relatively low to high values of α, the swarm moves from rotating as a rigid body to rotating as a mill, as shown in Figure 2.2. It should be noted that the force interaction law used by the authors (Equation 2.5) is slightly different than that in Equation 2.4.

The force balance is instead

$$m\frac{d\vec{w}_i}{dt} = \alpha\hat{\xi}_i - \beta\left|\left|\vec{w}_i\right|\right|^2\vec{w}_i + \sum_{j(j\neq i)}\left[V_{\mathrm{a}}'\left(\left|\left|\Delta\vec{z}_{i,j}\right|\right|\right)\frac{\Delta\vec{z}_{i,j}}{\left|\left|\Delta\vec{z}_{i,j}\right|\right|} + V_{\mathrm{r}}'\left(\left|\left|\Delta\vec{z}_{i,j}\right|\right|\right)\frac{\Delta\vec{z}_{i,j}}{\left|\left|\Delta\vec{z}_{i,j}\right|\right|}\right], \quad (2.5)$$

where $V_{\mathrm{a}}(\Delta\vec{z}_{i,j}) = C_a\mathrm{e}^{-\frac{\Delta\vec{z}_{i,j}}{l_a}}$ and $V_{\mathrm{r}}(\Delta\vec{z}_{i,j}) = C_r\mathrm{e}^{-\frac{\Delta\vec{z}_{i,j}}{l_r}}$; C_a, C_r, l_a, and l_r are parameters of the potential functions which can be adjusted to change the magnitude and range of V_a, V_r. The only difference, however, is in the drag term. Instead of directly scaling with the velocity of a particle, in Equation 2.5 the drag term is scaled with the velocity cubed. The resulting behaviors from Equation 2.5 depend not only on the form of the forces, but on the parameters which govern the equations. Hence, it is expected that changing these parameters would change the macroscopic behavior of the swarm.

2.4 Swarm Behaviors

As noted above, changes to the parameters in the potentials between elements determines the type of overall swarming pattern or stability the group will have, as seen in Figure 2.2. In broader terms, the VARP method is an example of a control scheme where the microscopic interactions of individuals give rise to perceived macroscopic behavior of the swarm, as was discussed in Section 1.1. The behavior of swarms obeying potentials such as those in Equation 2.5 has been classified according to the parameters governing the potentials in the work of D'Orsogna et al. (2006). This classification is based on the concept of *H-stability*: for a set of N interacting particles, the total potential energy U is said to be H stable if there exists a constant $B \geq 0$ such that $U \geq -NB$. Non–H-stable systems are also called catastrophic.

H-stability of the potential used in the VARP method is shown in Figure 2.3, as a function of $l = l_r/l_a$ and $C = C_r/C_a$. The phase transitions between stability define regions where the swarms exhibit particular macroscopic behaviors. In region I, for example, the particles form multiparticle clumps, and in each clump they move parallel to each other. On the other hand, swarms in region II form rotating rings with mean radius R dependent on the parameter values. Thus, we see how changing microscopic

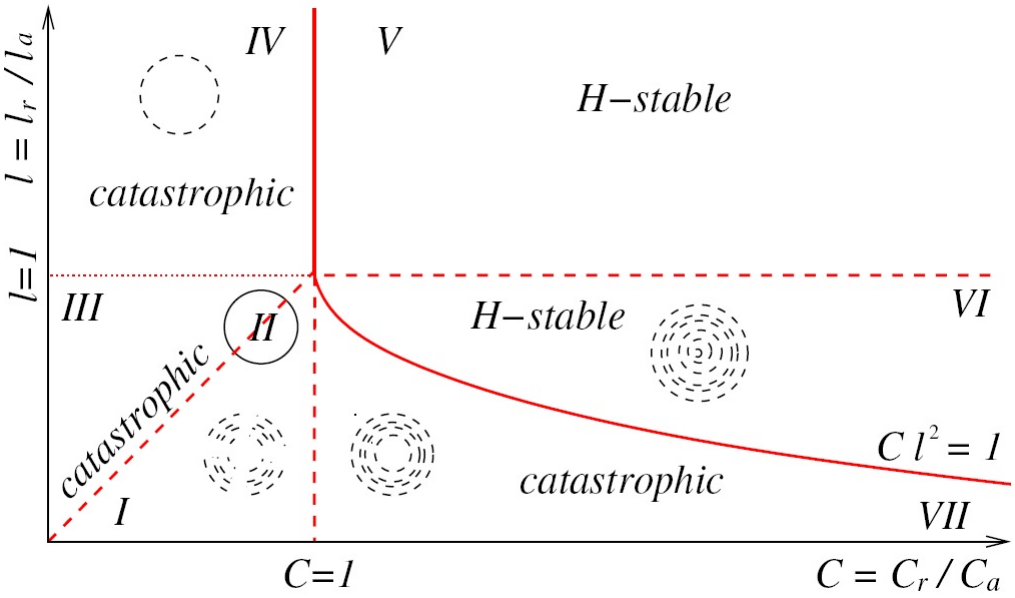

Figure 2.3 The figure depicts the phase transition diagram between regions of H-stability of swarms under the VARP model. Each region in the diagram has an associated macroscopic behavior that the swarm exhibits. The figure was obtained from D'Orsogna et al. (2006).

behavior in the swarm via adjustment of parameters governs the macroscopic behavior of the group. Moreover, H-stability is an analytical tool that sufficiently classifies these macroscopic behaviors.

Chapter 3

Control of Swarms Through the Abstraction Method (in Two Dimensions)

While the VARP method is an example of a control scheme where the microscopic interactions of individuals give rise to perceived macroscopic behavior of the swarm, it is possible to devise controls for individuals by first defining the macroscopic behavior or characteristics of the swarm. Such a method has been implemented by Belta and Kumar (2004). The approach has the following steps:

1. Characterize the swarm by its shape and position;
2. Define a map between the collective microscopic states of the swarm and the characterization in the previous step; and
3. Derive controls for individual elements based on the map in step 2.

The method outlined above relies on concepts from differential geometry, so we will first briefly introduce relevant definitions. Then, we will explain the control derivation and discuss the results and relevance of Belta and Kumar's work.

It must be made very clear that this chapter summarizes some of the original work of Belta and Kumar (2004).

3.1 Control Derivation

In their derivation of the control method via abstraction, Belta and Kumar (2004) assume that every member, or agent, of a group will be fully actuated: that is, the agent will be able to propel itself in any desired direction. Further, all movement will take place in $\mathbb{R}^2$. Each agent has a position vector $z_i \in Z_i = \mathbb{R}^2$ with respect to a single reference frame, with $i = 1, \ldots, N$. Let this frame be denoted as $\{M\}$. Thus, the *control* $u_i \in U_i = \mathbb{R}^2$ for each member is defined as

$$u_i = \dot{z_i}. \tag{3.1}$$

Equation 3.1 simply means that the instantaneous change of position of the element; that is, its velocity, is governed by a control vector representing the direction of heading and speed that the agent must have. The position and velocity of each agent in the swarm completely defines its state. When put together, all u_i and all z_i form a $2N$ dimensional space, since the vectors $u = (u_1, \ldots, u_N)$, $z = (z_1, \ldots, z_N)$ are each in $\mathbb{R}^{2N}$. Hence, each $z \in Z$ and $u \in U$ where we define

$$Z = \prod_{i=1}^{N} Z_i, \quad U = \prod_{i=1}^{N} U_i. \tag{3.2}$$

Further, because of Equation 3.1, $u = (\dot{z_1}, \ldots, \dot{z_N}) \in T_z Z$, the tangent space of Z at z, as given in Definition A.13. In general, for the tangent bundle TZ (Definition A.14) of the manifold Z, any vector field X_Z belonging therein ($X_Z \in TZ$) is defined by Belta and Kumar as a *behavior*.

With this notation, we can go on to describe the derivation of the control law.

3.1.1 Swarm Characterization

At any instant in time, the state of the swarm is given by some $z \in Z$ and its control by some $u \in U$. On a macroscopic level, the swarm can also be described by its gross shape, position and orientation. Hence, the state of the swarm can be described by assigning to each $z \in Z$ (through a map ϕ described in Section 3.2) some element in a differentiable manifold $(G \times S)$ where G captures the pose of the swarm and S its shape. We require that G and S to be differentiable manifolds because we will want to solve for u_i in terms of tangents on the lower-dimensional G and S. The goal of the derivation is to devise a way to control the shape and pose (position and orientation) of the swarm independently.

Since the positions of swarm elements are vectors in $\mathbb{R}^2$, each element r in the group of rotations $SO(2)$ can be represented by a matrix parameterized by a rotation angle θ so that

$$SO(2) \ni r(\theta) = \begin{pmatrix} \cos\theta & -\sin\theta \\ \sin\theta & \cos\theta \end{pmatrix}. \tag{3.3}$$

Since each element in $SO(2)$ is uniquely determined by θ, $SO(2)$ is homeomophic to $[0, 2\pi)$ via $\phi(r(\theta)) = \theta$. Since $[0, 2\pi)$ is homeomorphic to $SO(2)$, we can find a collection of charts (ϕ, U_i) such that $SO(2) = \cap_{i=1}^{\infty} U_i$. Further, for any $U_i \cap U_j \neq \emptyset$, $\phi \circ \phi^{-1}$ is the identity map, which is differentiable. Thus, by Definition A.9, $SO(2)$ is a differentiable manifold. Further, since $\det[r(\theta)] = 1$ for any θ, $r(\theta)$ is invertible. Namely,

$$r(\theta)^{-1} = \begin{pmatrix} \cos\theta & \sin\theta \\ -\sin\theta & \cos\theta \end{pmatrix}.$$

Note that the product of two elements in $SO(2)$ results in yet another element of $SO(2)$:

$$\begin{pmatrix} \cos\theta & -\sin\theta \\ \sin\theta & \cos\theta \end{pmatrix} \begin{pmatrix} \cos\psi & -\sin\psi \\ \sin\psi & \cos\psi \end{pmatrix} = \begin{pmatrix} \cos(\theta+\psi) & -\sin(\theta+\psi) \\ \sin(\theta+\psi) & \cos(\theta+\psi) \end{pmatrix}.$$

Similar results hold for inverses:

$$\begin{pmatrix} \cos\theta & \sin\theta \\ -\sin\theta & \cos\theta \end{pmatrix} \begin{pmatrix} \cos\psi & \sin\psi \\ -\sin\psi & \cos\psi \end{pmatrix} = \begin{pmatrix} \cos(\theta+\psi) & -\sin(\theta+\psi) \\ -\sin(\theta+\psi) & \cos(\theta+\psi) \end{pmatrix}.$$

Since sin and cos are infinitely differentiable, products of rotations and their inverses are smooth operations. Hence, $SO(2)$ is a real Lie group according to Definition A.18.

The set of translations T in $\mathbb{R}^2$ are also a Lie group. This is evident from the fact that for any $t \in T, v \in \mathbb{R}^2$,

$$t(v) = v + t',$$

where $t' \in \mathbb{R}^2$ and is unique to t. Because translations constitute vector addition in $\mathbb{R}^2$, they are a Lie group, as $\mathbb{R}^2$ is a manifold with the identity map for all its charts.

Together, $G = SO(2) \times T$ is a group consists of a pairs of rotations and translations. Here G forms a Lie group under the product topology where open sets in G are pairs of open sets in $SO(2)$ and T. By construction, G has

any topological and differentiable property shared by T and $SO(2)$ through a simple direct product. Hence, G is a Lie group.

Specifying the shape as a member of another group S, we have that the state of the swarm a is an element of the direct product

$$a \in A = G \times S. \tag{3.4}$$

Belta and Kumar (2004) require that the dimension n of A is independent of the number of robots N. Having loosely described G, and implicitly the map from Z to G, we can begin to define properties of the map $\phi : Z \to (G \times S)$.

3.1.2 Mapping

As described in Section 3.1.1, there are two ways of describing the state of a swarm: one microscopically via Z, and one macroscopically via $G \times S$. A map between these two spaces having certain properties (to be elaborated below) will make it possible to derive controls for agents in the group. With this in mind, let

$$\phi : Z \to G \times S \quad \text{with} \quad \phi(z) = a = (g, s) = (\phi_g, \phi_s). \tag{3.5}$$

The precise definition will be given in Section 3.2, but for now we focus on the properties of ϕ. We require that ϕ is a submersion (Definition A.17), and that it is invariant to permutations of the elements of the swarm. The importance that ϕ has a surjective differential will become important, because derivations for controls of elements in the swarm will rely on $d\phi$, the differential of ϕ (Definition A.16). Moreover, we want the controls for shape and pose to be independent. This means that ϕ_s is invariant under g; that is,

$$\phi(\bar{g}z) = (\bar{g}g, s). \tag{3.6}$$

In other words, if $\bar{g}$ is a translation, applying a translation to the swarm will affect only its pose and not its shape. Since all movement of the swarm takes place in $\mathbb{R}^2$, we can say with greater generality that $G \subset GL_2(\mathbb{R})$, where $GL_2(\mathbb{R})$ is the group of real-valued 2×2 invertible matrices. Equation 3.6 therefore shows that ϕ is left-invariant.

3.1.3 Abstraction Behavior

Belta and Kumar define an *abstract behavior* to be any vector field $T_A \in TA$. Note that the submersion condition for ϕ guarantees the surjectivity of $d\phi$

at any $z \in Z$. This means that for any $\dot{a} \in T_a A$, there will be a vector $\dot{z} \in T_z Z$ such that

$$d\phi \dot{z} = \dot{a}. \tag{3.7}$$

Recall that we require that the dimensionality of A is constant and does not scale with the size of the swarm N. As the dimensionality of the tangent spaces is the same as that of corresponding manifolds, in general, Equation 3.7 is an underdetermined system.

Belta and Kumar solve this system by minimizing the norm of $\dot{z}$ under the constraint of 3.7. They give the solution to $\min_{\dot{z}} \dot{z}^T \dot{z}$ under the constraint as

$$\dot{z} = d\phi^T \left(d\phi d\phi^T \right)^{-1} \dot{a}, \tag{3.8}$$

which is a solution to Equation 3.7.

Since ϕ is a submersion, $d\phi$ is a surjective map (and also a linear transformation), meaning that it is full-row rank, which implies that $\left(d\phi d\phi^T\right)$ is invertible. Writing $d\phi^T = \left(d\phi_g^T, d\phi_s^T\right), a^T = (g^T, s^T)$,

$$\begin{aligned} d\phi d\phi^T &= (d\phi_g, d\phi_s) \left(d\phi_g^T, d\phi_s^T \right) \\ &= \left(d\phi_g d\phi_g^T + d\phi_g d\phi_s^T, d\phi_s d\phi_g^T + d\phi_s d\phi_s^T \right). \end{aligned}$$

Now if we let $d\phi_g d\phi_s^T = 0$,

$$d\phi d\phi^T = \left(d\phi_g d\phi_g^T, d\phi_s d\phi_s^T \right). \tag{3.9}$$

Thus the assumption assures us that $d\phi d\phi^T$ cab be decomposed into g and s components. Hence Equation 3.8 becomes

$$\dot{z} = d\phi_g^T (d\phi_g d\phi_g^T)^{-1} \dot{g} + d\phi_s^T (d\phi_s d\phi_s^T)^{-1} \dot{s}, \tag{3.10}$$

which is a general form of the control for the entire swarm. To get controls for each individual element z_i, the vector in Equation 3.10 is projected onto z_i. This projection is naturally dependent on the choice of ϕ.

3.2 Results

In their work, Belta and Kumar define a map ϕ having the required properties. The map ϕ is based on physical qualities of the swarm. Particularly,

$$\phi(z) = ((R, \mu), (s_1, s_2)), \tag{3.11}$$

where

$$\mu = \frac{1}{N}\sum_{i=1}^{N} z_i \in \mathbb{R}^2, \tag{3.12}$$

which is a position average of the swarm. Further, if we write $z_i = (x_i, y_i)$, $R \in SO(2)$ is a rotation that is defined by the equation

$$\sum_{i=1}^{N} x_i y_i = 0, \tag{3.13}$$

which can be parameterized by a single variable θ. We can then define the position of each member of the swarm with R, μ by defining r_i where

$$r_i = (x_i, y_i)^T = R^T(z_i - \mu), i = 1, \ldots, N. \tag{3.14}$$

The shape variable $s = (s_1, s_1)$ is defined by

$$\begin{aligned} s_1 &= \frac{1}{N-1}\sum_{i=1}^{N} x_i^2, \\ s_2 &= \frac{1}{N-1}\sum_{i=1}^{N} y_i^2. \end{aligned} \tag{3.15}$$

Thus, the shape variable is a measurement of the distribution of elements in the swarm along the axes of the world frame $\{M\}$.

3.2.1 The Map Differential $d\phi$

As can be seen in Equations 3.8 and 3.10, the derivation of the individual control law requires that we have the differential of the map ϕ $d\phi$ and also $d\phi^T$. As seen in Definition A.16, a differential is defined as a map between the tangent spaces of two manifolds. In local coordinates, we see that ϕ is a function of μ, θ, s_1, and s_2, so that $d\phi = (d\mu, d\theta, ds_1, ds_2)$. To find these differentials, it is useful to introduce some useful notation giving rise to a more natural decomposition. We let

$$\begin{aligned} E_1 &= \begin{bmatrix} 0 & 1 \\ 1 & 0 \end{bmatrix}, \\ E_2 &= \begin{bmatrix} 1 & 0 \\ 0 & -1 \end{bmatrix}, \\ E_3 &= \begin{bmatrix} 0 & -1 \\ 1 & 0 \end{bmatrix}, \end{aligned} \tag{3.16}$$

$$
\begin{aligned}
H_1 &= I_2 + R^2 E_2, \\
H_2 &= I_2 - R^2 E_2, \\
H_3 &= R^2 E_1,
\end{aligned} \tag{3.17}
$$

using the parameterization for R in Equation 3.3. All of the H_i matrices are symmetric, which will be important in finding $d\phi^T$. This notation in general is useful when dealing with the position vectors of members of the swarm under the transformation yielding r_i (Equation 4.2). First we note that

$$\sum x_i y_i = 0 \Leftrightarrow 2\sum x_i y_i = 0.$$

Observe that

$$
\begin{aligned}
2\sum x_i y_i &= \sum (x_i, y_i)(y_i, x_i)^T && (3.18)\\
&= \sum (R^T(z_i - \mu))^T (y_i, x_i)^T && (3.19)\\
&= \sum (z_i - \mu)^T R E_1 (x_i, y_i)^T. && (3.20)
\end{aligned}
$$

Further, since $(x_i, y_i)^T = R^T(z_i - \mu)$, and $RR^T = I$, the sum can be expressed as $\sum (z_i - \mu)^T R E_1 R^T (z_i - \mu)$. A simple calculation shows that $RE_1R^T = R^2E_1 = H_3$ so that

$$2\sum x_i y_i = \sum (z_i - \mu)^T H_3 (z_i - \mu) = 0. \tag{3.21}$$

This conversion is then used to find the differentials of s_1 and s_2, which in turn take on similar forms

$$
\begin{aligned}
s_1 &= \frac{1}{2(N-1)} \sum_{i=1}^{N} (q_i - \mu)^T H_1 (q_i - \mu), \\
s_2 &= \frac{1}{2(N-1)} \sum_{i=1}^{N} (q_i - \mu)^T H_1 (q_i - \mu).
\end{aligned} \tag{3.22}
$$

The condition expressed in Equation 3.21 gives a solution for θ. If we let $z_i - \mu = (a_i, b_i)^T$ and observe that

$$H_3 = \begin{bmatrix} 0 & \cos 2\theta \\ \cos 2\theta & \sin 2\theta \end{bmatrix},$$

Equation 3.21 becomes

$$\sum_{i=1}^{N} (a_i^2 - b_i^2) \cos 2\theta + \sum_{i=1}^{N} (a_i b_i) \sin 2\theta = 0,$$

which implies that

$$\frac{-\sum_{i=1}^{N}(a_i^2 - b_i^2)}{\sum_{i=1}^{N}(a_i b_i)} = \frac{\sin 2\theta}{\cos 2\theta} = \tan 2\theta,$$

which is a unique solution for θ.

3.2.2 Spanning Rectangle

As mentioned above, μ can be viewed as the *centroid*, or "average" center, of the swarm. In a similar physical vein, Γ is the inertia of the system where

$$\Gamma = -(N-1)E_3\Sigma E_3, \tag{3.23}$$

with

$$\Sigma = \frac{1}{N-1}\sum_{i=1}^{N}(z_i - \mu)(z_i - \mu)^T.$$

To see why this is so, we only need to observe the formula for inertia I of an N body, point-mass system,

$$I = \sum_{i=1}^{N} m_i t_i^2, \tag{3.24}$$

where m_i is the mass of the element i and t_i is the distance between the centroid of the system to the location of element i. The vector $(z_i - \mu)$ extends from the centroid to z_i, and $(z_i - \mu)(z_i - \mu)^T$ is the inner product of this vector with itself; that is, the squared distance from the centroid to the element.

If $\{W\}$ is the virtual frame with pose $g = (R, \mu)$ in $\{M\}$, then r_i, as defined in Equation 3.14, is the expression of $z_i - \mu$ in the virtual frame, so that the inertia tensor of the system of points r_i in $\{W\}$ is diagonal. $(N-1)s_1$ and $(N-1)s_2$ are the eigenvalues of the tensor and are related to the distribution of robots along the axis of virtual frame $\{W\}$. Further, these eigenvalues present an upper bound on the distribution of the positions of elements in the swarm, since for any $i = 1, \ldots, N$,

$$|x_i| \leq \sqrt{(N-1)s_1}, \quad |y_i| \leq \sqrt{(N-1)s_2}.$$

This result shows that, based on the map ϕ, the controls for each element of the swarm cause the ensemble of agents to move within a rectangle whose with and height are dependent on parameters of ϕ. By controlling

these parameters and others associated with the movement of the swarm elements, Belta and Kumar demonstrate the capabilities of the abstraction method. They are able to drive a group of ten robots through a tunnel by implementing their controls in numerical simulations, as seen in Figure 3.1.

3.3 Relevance of the Abstraction Method

The abstraction method presented in this chapter is related to the VARP method described in the previous chapter, with notable differences. First, given a large number of robots, the abstraction method allows for a solution of the motion-generation/control problems on a smaller dimensional space than $\mathbb{R}^{2N}$. Second, the dimension of the control problem is independent of the number of agents and independent of the possible ordering of the robots. Finally, the abstraction method is one in which the macroscopic swarm behavior dictates the controls of individual elements, the inverse of the effect of the VARP method. Just as in the VARP approach, behaviors using abstraction control can be characterized according to parameters in the model, as we saw in the case of the bounds on the swarm distribution using the rectangular box.

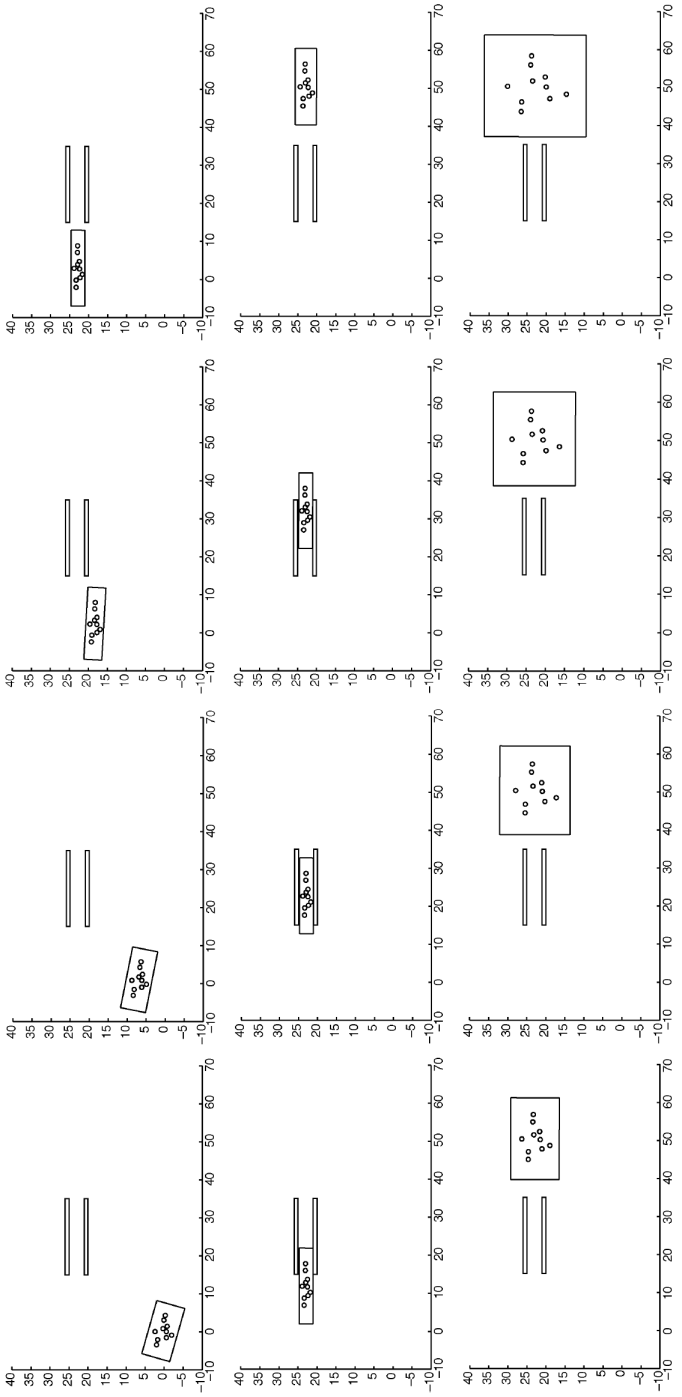

Figure 3.1 By controlling the parameters that determine the dimensions and position of the spanning rectangle, the swarm is guided through a narrow tunnel. The figure obtained from Belta and Kumar (2004).

Chapter 4

New Control Law

As outlined in Chapter 2, the VARP method generates a control law inducing the macroscopic behaviors depicted in Figure 2.3. These behaviors are most generally characterized by circular motion about a central point. Particularly, the regime of H-stability generates behavior of disk-like formations revolving about a central point (Figure 2.2).

We want to design a control law which mimics the H-stability behavior achieved through the VARP method. In the language of Belta and Kumar, we want to come up with a function ψ which maps from the space of coordinates of all members of a swarm to a manifold which characterizes the swarm in a global way. These global characteristics, defined more precisely in Sections 4.1, 4.2, and 4.3, are limited to the swarm having radial symmetry and a uniform distribution on a disk. These two characteristics are very much a first-order approximation to the behavior exhibited in Figure 2.2.

Naturally, one would note that these two specifications do not necessarily guarantee the nature of the motion the swarm elements; it is conceivable that one could have radial symmetry and a uniform-disk distribution without circular motion about the center of the swarm. However, motion observed under the VARP method is the result of the "self-propulsion" term which works to cause the entire swarm to move about a center point in a mill-like pattern. The difficulty in reproducing this result using the abstraction method is that the abstraction method fist defines global characteristics which subsequently produce individual controls, and not the other way around. Further, limiting the control law to tracking only two global characteristics would make the analysis of results and the behavior due to the control easier and hence more appropriate for this work. We thus define

the map ψ as

$$\psi : Z \to (A, X),$$

such that $\psi(z) = (\alpha, \chi^2) \in A \times X$, with Z defined in Equation 3.2. Here, α captures the radial symmetry of the swarm, whereas χ^2 captures how the distribution of the swarm compares to a uniform distribution on a disk. The differentials of ψ (Section 4.4) will yield a control law for the individual elements, as given in Equation 3.8, provided $d\psi$ is of full-row rank. With this introduction, we begin the precise definition of ψ.

4.1 Radial Symmetry

We wish to find the center of the swarm, and this is done by finding the average of all positions of elements in the group. Let

$$\mu = \frac{1}{N} \sum_{i=1}^{N} z_i, \tag{4.1}$$

where z_i is the Eulerian coordinate of the i^{th} element and N is the number of elements in the swarm. Hence, μ is the centroid of the system. Since we are concerned first with radial symmetry and the disk-like structure of the system, we transform each z_i by a translation, defining

$$r_i = z_i - \mu. \tag{4.2}$$

As explained above, we wish to preserve radial symmetry, so we define a way to measure it, namely,

$$\alpha = \sum_{i=1}^{N} r_i. \tag{4.3}$$

If indeed the swarm Z is radially symmetric, we will have $\alpha = 0$. Now, we move to a characterization of whether Z is a disk.

4.2 Uniform Distribution on a Disk

We let

$$R = \max\{r_i\}, \tag{4.4}$$

so that, ideally, the swarm is to be uniformly distributed within a circle with radius R centered at μ.

It is necessary to take a moment and explain how uniform distribution works on a disk. Under a simple transformation relative to an arbitrary axis, we can express each coordinate r_i as a pair (R_i, θ_i) where $R_i = ||r_i||$ and θ_i is the angle of $r_i = (x_i, y_i)^T$ given by $\arctan(y_i/x_i)$. Because of the geometry of the circle, we cannot simply require that $R_i \sim U[0, R]$ and $\theta_i \sim U[0, 2\pi]$. More precisely, observe that the probability of the radius R_i of a swarm particle being less than a given a is

$$P(R_i \leq a) = \frac{\pi a^2}{\pi R^2},$$

which implies that the probability of R_i equaling a is

$$P(R_i = a) = \frac{\partial}{\partial a}\left(\frac{\pi a^2}{\pi R^2}\right) = \frac{2\pi a}{\pi R^2} = \frac{2a}{R^2},$$

so that the distribution of R_i is certainly not uniform, for it depends on the value of a. However, this problem is eliminated if we consider R_i^2. Namely,

$$\begin{aligned} P(R_i^2 \leq a^2) =& \frac{\pi a}{\pi R^2} \\ \Rightarrow P(R_i^2 = a^2) =& \frac{\partial}{\partial a^2}\left(\frac{\pi a^2}{\pi R^2}\right) = \frac{\pi}{\pi R^2} = \frac{1}{R^2} \end{aligned}$$

and so $R_i^2 \sim U\left[0, R^2\right]$. Hence, we can conclude that if $(R_i^2, \theta_i) \sim U[0, R^2] \times U[0, 2\pi]$, then $\{r_i\}$ is uniformly distributed on a disk with center μ and radius R.

4.3 The χ^2 Measurement

A useful way of measuring how a sample compares to a hypothetical distribution is the χ^2-test. Here, if we divide the region $[0, R^2] \times [0, 2\pi]$ into four equal subregions $Q_1, \ldots Q_4$, the χ^2 statistic is

$$\chi^2 = \sum_{j=1}^{4} \frac{(f_j - N\pi_j)^2}{N\pi_j}, \tag{4.5}$$

where f_j is the observed frequency of samples in region Q_j and π_j is the hypothetical probability of a sample being that region (which in this case is $1/4$) and N is the number of samples. If we let $g(r_i) = (R_i^2, \theta_i)$, we can count the number of samples in Q_j in the following way:

$$f_j = \sum_{i=1}^{N} r_i^T \hat{f}_{ji} r_i, \tag{4.6}$$

where

$$\hat{f}_{ji} = \begin{cases} \begin{pmatrix} 0 & 0 \\ 0 & 0 \end{pmatrix} & \text{if } g(r_i) \notin Q_j, \\ \begin{pmatrix} 1/(2x_i^2) & 0 \\ 0 & 1/(2y_i^2) \end{pmatrix} & \text{if } g(r_i) \in Q_j. \end{cases}$$

It is important to note the significance of the form of Equation 4.6. After all, we could have done something as simple as

$$f_j = \sum_{i=1}^{N} \chi_{Q_j}(g(r_i))$$

where χ_{Q_j} is the indicator function of the set Q_j, since this form is actually easier to implement. But the difficulty is that we not only care about χ^2 but also $d\chi^2$, and it is difficult to define the derivative of an indicator function in a meaningful way. On the other hand, given Equation 4.6,

$$\begin{aligned} \frac{\partial f_j}{\partial z_i} &= \frac{\partial}{\partial z_i} \sum_{i=1}^{N} r_i^T \hat{f}_{ji} r_i \\ &= \sum_{i=1}^{N} \frac{\partial}{\partial z_i} (z_i - \mu)^T \hat{f}_{ji} (z_i - \mu) \\ &= I^T \hat{f}_{ji} (z_i - \mu) + (z_i - \mu)^T \hat{f}_{ji} I \\ &= \hat{f}_{ji} (z_i - \mu) + (z_i - \mu)^T \hat{f}_{ji} \\ &= \hat{f}_{ji} r_i + r_i^T \hat{f}_{ji}. \end{aligned}$$

Immediately we can see that the dimensionality of the above expression is not consistent, as $\hat{f}_{ji} r_i$ is a column vector, whereas $r_i^T \hat{f}_{ji}$ is a row vector. This inconsistency is not entirely disturbing, as f_j is a scalar value resulting from the products of matrix elements. We can reconcile this difficulty, recognizing that $(\hat{f}_{ji} r_i)^T = r_i^T \hat{f}_{ji}$ so that the entries in the two vectors are the same. Hence, we set

$$\frac{\partial f_j}{\partial z_i} = 2 r_i^T \hat{f}_{ji}, \tag{4.7}$$

since this preserves the absolute value of the partial derivative. Thus,

$$\begin{aligned} \frac{\partial \chi^2}{\partial z_i} &= \frac{\partial}{\partial z_i} \sum_{j=1}^{4} \frac{(f_j - N\pi_j)^2}{N\pi_j} = \sum_{j=1}^{4} \frac{\partial}{\partial z_i} \frac{(f_j - N\pi_j)^2}{N\pi_j} \\ &= \sum_{j=1}^{4} \frac{2(f_j - N\pi_j)}{N\pi_j} \frac{\partial f_j}{\partial z_i} \\ &= \sum_{j=1}^{4} \frac{2(f_j - N\pi_j)}{N\pi_j} 2 r_i^T \hat{f}_{ji} = \sum_{j=1}^{4} \frac{4(f_j - N\pi_j)}{N\pi_j} r_i^T \hat{f}_{ji}. \end{aligned}$$

Equipped with $\partial\chi^2/\partial z_i$ we are now able to find the differential of ψ and so derive control law for the swarm.

4.4 The Differential $d\psi$

In this section we find find $d\psi$, as it is required for the derivation of the control law given in Equation 3.8. The formal definition of a differential is given in Definition A.16. However, because of the linear properties of derivatives, the differential of a map is a linear transformation from one tangent space to another. The entries in the matrix encoding this linear transformation are the partial derivatives of the function, in this case ψ, with respect to coordinates given by the coordinate chart of the map. Since $Z = \mathbb{R}^{2N}$, Z has global coordinates, so that $d\psi$ is simply the Jacobian of ψ:

$$d\psi = \begin{pmatrix} \frac{\partial\alpha}{\partial z_1} & \cdots & \frac{\partial\alpha}{\partial z_{2N}} \\ \frac{\partial\chi^2}{\partial z_1} & \cdots & \frac{\partial\chi^2}{\partial z_{2N}} \end{pmatrix}.$$

Having already obtained the partial of χ^2 with respect to z_i, we set

$$\frac{\partial\chi^2}{\partial z_i} = M_i = \sum_{j=1}^{4} \frac{4(f_j - N\pi_j)}{N\pi_j} r_i^T \hat{f}_{ji} = \sum_{j=1}^{4} \frac{4(f_j - N\pi_j)}{N\pi_j} \left(\frac{1}{2x_i}, \frac{1}{2y_i}\right).$$

From the above expression, we can see that M_i depends on the inverses of the coordinates of z_i as well as the number of elements in the quadrant Q_k that z_i belongs to. The differential of α is calculated similarly:

$$\begin{aligned} \frac{\partial\alpha}{\partial z_i} &= \frac{\partial}{\partial z_i}\sum_{i=1}^{N} r_i = \frac{\partial}{\partial z_i}\sum_{i=1}^{N}(z_i - \mu) \\ &= \sum_{i=1}^{N}\frac{\partial}{\partial z_i}(z_i - \mu) \\ &= I. \end{aligned}$$

With expressions for $d\chi^2$ and $d\alpha$, we can express $d\psi$ as the matrix

$$d\psi = \begin{pmatrix} I & \cdots & I \\ M_1 & \cdots & M_N \end{pmatrix}. \tag{4.8}$$

4.5 The Control Law

As discussed earlier, the control law for the swarm is directly dependent on the map ψ, or more precisely on its differential (Equation 3.8). In this section we use Equation 3.8 to derive the control law for the swarm.

With the map $\psi : Z \to A \times X$, the differential of ψ is a linear map from the tangent bundle of Z to the tangent bundle of A, namely if $\dot{z}$ is the derivative of a parametrized curve on Z,

$$d\psi\dot{z} = (\dot{\alpha}, \dot{\chi^2}). \tag{4.9}$$

Since $d\psi$ is a matrix, the above expression is a linear system, so that if $d\psi$ is full row rank, we can use the expression in Equation 3.8 to find $\dot{z}$ *in terms of* $(\dot{\alpha}, \dot{\chi^2})$. In other words, the control problem is no longer solved in $\mathbb{R}^{2N}$ but rather in $A \times X = \mathbb{R}^2$. Put in yet another way, the behavior of all N elements in the swarm is determined solely by the values of the derivatives of α and χ^2.

Letting

$$M_i = (m_i \ n_i), \ \sum_{i=1}^{N} M_i = (a \ b), \ \sum_{i=1}^{N} M_i M_i^T = c, \ D = c - \frac{a^2}{N} - \frac{b^2}{N},$$

calculation shows that

$$d\psi^T(d\psi d\psi^T)^{-1} = \begin{pmatrix} \frac{1}{N} + \frac{a^2}{N^2D} - \frac{am_1}{ND} & \frac{ab}{N^2D} - \frac{bm_1}{ND} & \frac{-a}{ND} + \frac{m_1}{D} \\ \frac{ab}{N^2D} - \frac{an_1}{ND} & \frac{1}{N} + \frac{b^2}{N^2D} - \frac{bn_1}{ND} & -\frac{b}{ND} + \frac{n_1}{D} \\ & \vdots & \\ \frac{1}{N} + \frac{a^2}{N^2D} - \frac{am_N}{ND} & \frac{ab}{N^2D} - \frac{bm_N}{ND} & \frac{-a}{ND} + \frac{m_N}{D} \\ \frac{ab}{N^2D} - \frac{an_N}{ND} & \frac{1}{N} + \frac{b^2}{N^2D} - \frac{bn_N}{ND} & -\frac{b}{ND} + \frac{n_N}{D} \end{pmatrix}. \tag{4.10}$$

And since $\dot{q} = d\psi^T(d\psi d\psi^T)^{-1}\dot{a}$, the individual control laws are given by

$$\begin{aligned} \dot{z_i} \ = \ & \begin{pmatrix} \frac{1}{N} + \frac{a^2}{N^2D} - \frac{am_i}{ND} \\ \frac{ab}{N^2D} - \frac{an_i}{ND} \end{pmatrix} \dot{\alpha_1} + \begin{pmatrix} \frac{ab}{N^2D} - \frac{bm_i}{ND} \\ \frac{1}{N} + \frac{b^2}{N^2D} - \frac{bn_i}{ND} \end{pmatrix} \dot{\alpha_2} \\ & + \begin{pmatrix} \frac{-a}{ND} + \frac{m_i}{D} \\ -\frac{b}{ND} + \frac{n_i}{D} \end{pmatrix} \dot{\chi^2}. \end{aligned} \tag{4.11}$$

Equation 4.11 is decomposed according to contributions from the values of derivatives of the two parameters (α has two components). The numerical implementation of the results depends on how we choose to define

$\dot{\alpha}$ and $\dot{\chi^2}$ based on values of α and χ^2. Section 4.6 details the way these derivatives are defined.

4.6 Implementation and Results

To see the behaviors induced by the control law in Equation 4.11, we use a numerical implementation of the ODE composing the law. Here, the derivatives in question are $\dot{z_i}, \dot{\alpha}$, and $\dot{\chi^2}$, denoting the derivatives of *parameterized* curves, where the path of z_i is determined by the paths of α and χ^2. The parameterization of α and χ^2 is defined with respect to time; that is, $\alpha = \alpha(t), \chi^2 = \chi^2(t)$, so that $\dot{\alpha} = d\alpha/dt$ and $\dot{chi^2} = d\chi^2/dt$. This means that $z_i = z_i(t)$, and $\dot{z_i} = dz_i/dt$. For the sake of simplicity, the parameterized path for α and χ^2 is defined by the goal conditions α_g and χ^2_g, so that the respective derivatives are just weighted differences between the current and goal values.

Numerical experiments like the one done here rely on a discretization of the domain and range of the ODE, that is, they rely on a discretization of the parameter t and values for z_i. The implementation of this method relies on simple forward-Euler approach, given by

$$z_i^{n+1} = z_i^n + \dot{z_i^n} dt, \tag{4.12}$$

where the superscript indicates the discretized timestep. Given any time n, we have the global state of the swarm $z^n = (z_1^n \ z_2^n \ \dots z_N^n)^T$, so that we find both α and χ^2 for that time. Then, using the goal conditions for the swarm α_g, χ^2_g we calculate the derivatives $\dot{\alpha}, \dot{\chi^2}$ according to the expressions

$$\dot{\alpha_1} = k_{\alpha_1}(\alpha_{1,g} - \alpha_1), \tag{4.13}$$

$$\dot{\alpha_2} = k_{\alpha_2}(\alpha_{2,g} - \alpha_2), \tag{4.14}$$

$$\dot{\chi^2} = k_{\chi^2}(\chi^2_g - \chi^2), \tag{4.15}$$

where $k_{\alpha_1}, k_{\alpha_2}, k_{\chi^2}$ are positive nonzero constants. Simulations were run for $k_{\alpha_1} = 1, k_{\alpha_2} = 1, k_{\chi^2} = 1000$ and $dt = 0.01$. The constant for $\dot{\chi^2}$ is of much greater magnitude than the other two, because $O(1000)$ was the order magnitude which produced tractable behaviors. With smaller constants the initial conditions remained constants, and with greater order magnitudes positions of elements in the swarm became unbounded. The initial condition for the first simulation consisted of 100 uniformly distributed points on the square $[0, 3] \times [0, 3]$. The initial condition and final conditions after 1000 timesteps is given in Figure 4.1.

There were four designated quadrants for measuring the χ^2 distribution, given in the form of a direct product of the angle and squared radius range

$$\begin{aligned} QI &= [0\pi] \times [R^2/2, R^2] \\ QII &= [0\pi] \times [0, R^2/2] \\ QIII &= [-\pi 0] \times [0, R^2/2] \\ QIV &= [-\pi, 0] \times [R^2/2, R^2]. \end{aligned}$$

Five clusters form, and it seems that the arrangement of the outer ones might suggest the existence of an internal axis. It is also important to note that although the α parameter was 0 throughout the simulation, the χ^2 value never approached zero, as can be seen in Figure 4.2. The oscillations are due to the constant change of positions of the inner cluster. The outer clusters stay stationary as time increases.

4.6.1 Uniform Disk Initial Condition

We test the performance of the control law in the case where the initial condition is composed of 1000 points uniformly distributed on the unit disk, as seen in Figure 4.3, to see if the code implementing the control law could detect if the swarm did achieved a uniform disk distribution with radial symmetry. If the code works properly, such initial conditions would cause the simulation to terminate almost immediately, and the original positions for the swarm elements will not be disturbed.

After fourteen numerical timesteps with the above parameters, the desired goal of having $\alpha \approx 0$ and $\chi^2 \approx 0$ are achieved, with the final configuration being as seen in Figure 4.4.

The fact that the algorithm arising from the control law recognizes data which has a uniform disk distribution shows that the algorithm works on a basic level. However, the true test comes when the initial condition has a distribution different than the one which is the goal of the law.

4.6.2 Uniform Square Initial Condition

This part of the simulations is done with an initial condition consisting of 1000 points uniformly distributed on a unit square centered at $(0.5, 0.5)$. We observe a more dynamic behavior, as seen in Figure 4.5. Most notable of the features of the system in Figure 4.5 is the formation of five distinct accumulations of swarm elements: four formations along the diagonals of

the coordinate axes and a central, radially symmetric formation. The rest of this section will explain how the control law generates these dynamics.

The Initial Stage

What is referred to here as the *initial stages* are the system states for time-steps with $n < 1000$. The early stage of the control solution is characterized by a lack of the diagonally aligned groups. Further, most elements are contained in QII and $QIII$, since there are relatively low number of elements that are outside of the original formation. The occurrence and accumulation of such outliers is a numerical artifact of the implementation of the control law. It is appropriate to note that for this initial condition type the parameter $\alpha \approx 0$ so that $\dot{\alpha} \approx 0$. On the other hand, the group definitely does not have a uniform disk distribution, so that $\dot{\chi^2} << 0$ (since $\chi_g^2 = 0$). Hence, the control law is given by

$$\dot{z} = \begin{pmatrix} \frac{-a}{ND} + \frac{m_i}{D} \\ -\frac{b}{ND} + \frac{n_i}{D} \end{pmatrix} \dot{\chi^2} = \begin{pmatrix} \frac{Nm_i - a}{ND} \\ \frac{Nn_i - b}{ND} \end{pmatrix} \dot{\chi^2}. \tag{4.16}$$

Recall that

$$(m_i\,,\, n_i) = 4\frac{(f_j - N\pi_j)}{N\pi_j}\left(\frac{1}{2x_i}\,,\, \frac{1}{2y_i}\right),$$

and that

$$a = \sum_{i=1}^{N} m_i \quad b = \sum_{i=1}^{N} n_i.$$

As might be noted, the symmetry of the swarm should imply that $a, b \approx 0$, since both are essentially summations over the coordinates of all points in the group. However, if there is some small x_i or y_i that does not have an exact mirror image, then $\frac{1}{x_i}$ would weigh the entire summation greatly, forcing its absolute value to blow up. And it is this precise phenomenon that causes the formation of outliers. For the control law, we have

$$\dot{z} = \begin{pmatrix} \frac{Nm_i - a}{ND} \\ \frac{Nn_i - b}{ND} \end{pmatrix} \dot{\chi^2} = \begin{pmatrix} \frac{(N-1)m_i - \sum_{j\neq i} m_j}{ND} \\ \frac{(N-1)n_i - \sum_{j\neq i} n_j}{ND} \end{pmatrix}. \tag{4.17}$$

Hence we see that the occasional elements whose x_i or y_i coordinates become very small induce a great shift in the corresponding control velocity, as

$$(N-1)m_i >> \sum_{j\neq i} m_j \Rightarrow (N-1)m_i - \sum_{j\neq i} m_j \approx (N-1)m_i.$$

In this manner we see that elements which are found close to the axes centered at μ are flung far out from the initial group in the consequent timestep. It is important to note that this process, although determined by the control law, is essentially random, as the initial positions of the group elements are generated randomly. This is confirmed by observing the values for a and b over the course of the simulation, as pictured in Figure 4.6.2, since the spikes in the graphs correspond to elements with coordinates close to zero. It should be observed that each spike is quickly reduced, which accounts for the control law correcting the position as described above.

The Evolved Stage

The evolved stage of the solution is characterized by the formation and separation of the diagonal groups. The dynamics of the evolved stage are determined by the distribution of elements in the four quadrants and the positions of group elements. First, we observe that as in the initial stage of solution, the values of a and b tend to quickly correct themselves from one timestep to the next (Figure 4.6.2). Hence, over time, a and b do not affect the behavior of swarm elements. Thus, the direction of control for each element is simply determined by $(m_i\,,\,n_i)\dot{\chi}^2$, as the product $ND > 0$.

In the evolved stage of the solution, there are more points accumulated further away from the center of the group μ so that there are more elements in QI and QIV. Hence, f_1 and f_4 are greater than during the initial stage. However, since the bulk of the group is still in QII and $QIII$, the coefficients

$$\frac{f_1 - N\pi_1}{N\pi_1},\ \frac{f_4 - N\pi_4}{N\pi_4} < 0.$$

And since for elements in QI and QIV

$$m_i = 4\frac{(f_{1\text{or}4} - N\pi_{1\text{or}4})}{N\pi_{1\text{or}4}}\frac{1}{2x_i}\ \ n_i = 4\frac{(f_{1\text{or}4} - N\pi_{1\text{or}4})}{N\pi_{1\text{or}4}}\frac{1}{2y_i},$$

$(m_i\,,\,n_i)$ have opposite signs of $(x_i\,,\,y_i)$. But because $\dot{\chi}^2 < 0$, $(m_i\,,\,n_i)\dot{\chi}^2$ has the same signs as $(x_i\,,\,y_i)$ for elements in QI and QIV. For elements in $QII, QIII$, signs of $(m_i\,,\,n_i)\dot{\chi}^2$ are opposite of $(x_i\,,\,y_i)$. Thus, we can see why the the outer groups align with the diagonals: only with such an approximate position are influences of m_i and n_i equalized and keep them moving away from μ. On the other hands, elements in $QII, QIII$ are attracted to μ but upon reaching proximity to one of the axes they are shot

out. If their distance from μ is greater than $R^2/2$, then they join the outer diagonal groups. However, as R^2 grows with time due to the repulsion of the outer groups from μ this becomes increasingly unlikely. This dynamic is demonstrated in Figure 4.8, where the green circle is of radius $R^2/2$, thereby denoting the boundary between $QI \cup QIV$ and $QII \cup QIII$.

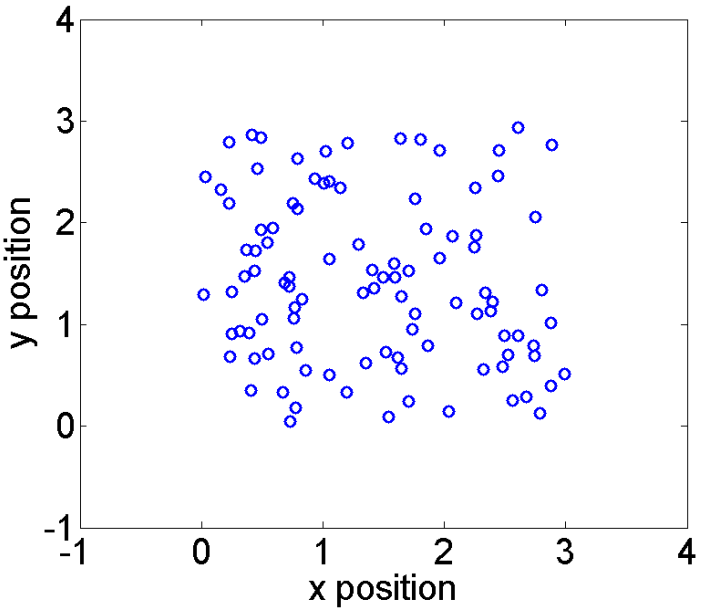

a. Initial condition consisting of 100 points uniformly distributed on a square with side length 3, centered at $(1.5, 1.5)$.

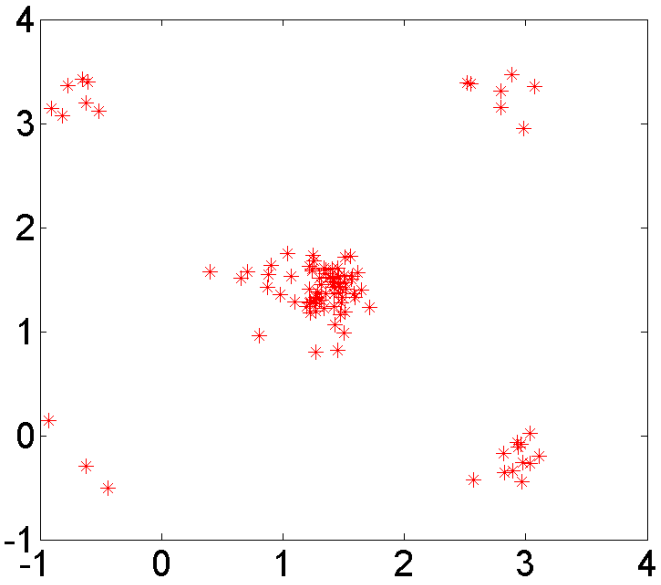

b. Depicted is the swarm distribution after 1000 timesteps. Five clusters form, and the arrangement of the four outer clusters might suggest the existence of an internal axis, as they are aligned along the diagonals.

Figure 4.1 Initial and final conditions for 100 points over 1000 timesteps.

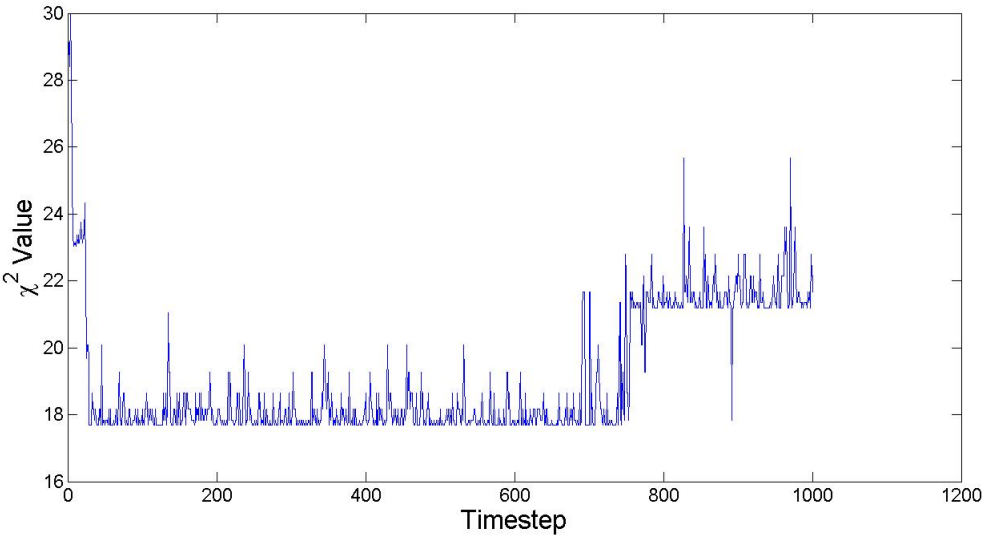

Figure 4.2 Plotted are χ^2 values for 1000 timesteps for an initial condition of 100 points uniformly distributed on a square with side length 3, centered at $(1.5, 1.5)$. Note that the value of the parameter never approaches 0 and exhibits very discontinuous behavior.

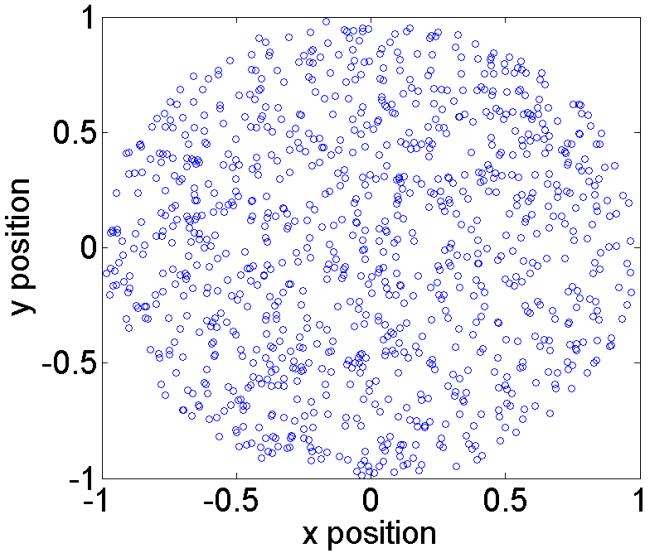

Figure 4.3 Shown is an initial condition consisting of 1000 points uniformly distributed on the unit disk.

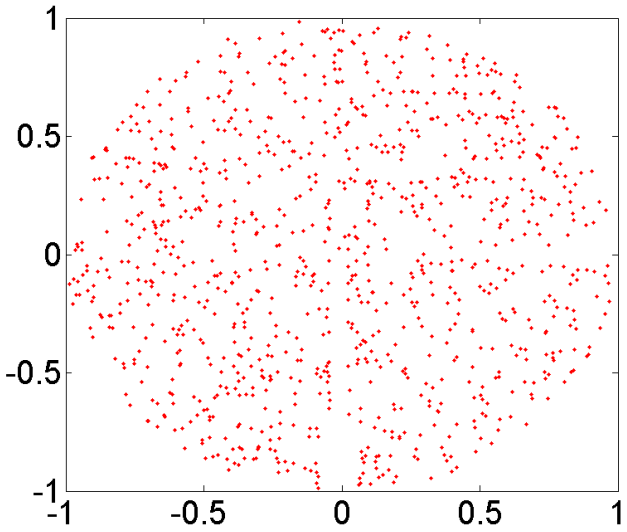

Figure 4.4 A system initially consisting of 1000 points uniformly distributed on the unit disk has the above final condition ($n = 11$). The algorithm terminates without making major changes to the initial condition.

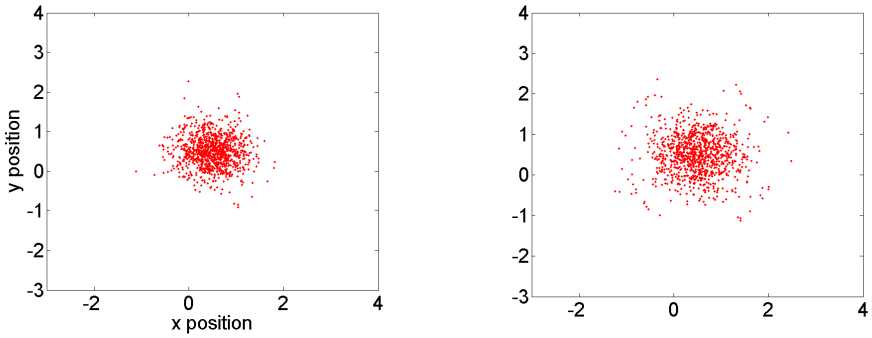

a. $n = 1000$ **b.** $n = 2000$

c. $n = 3000$ **d.** $n = 4000$

Figure 4.5 Progressive results for initial condition of 1000 points on the unit square. Note the emergence of five distinct clusters and the radial boundary separating the center cluster from the outer ones.

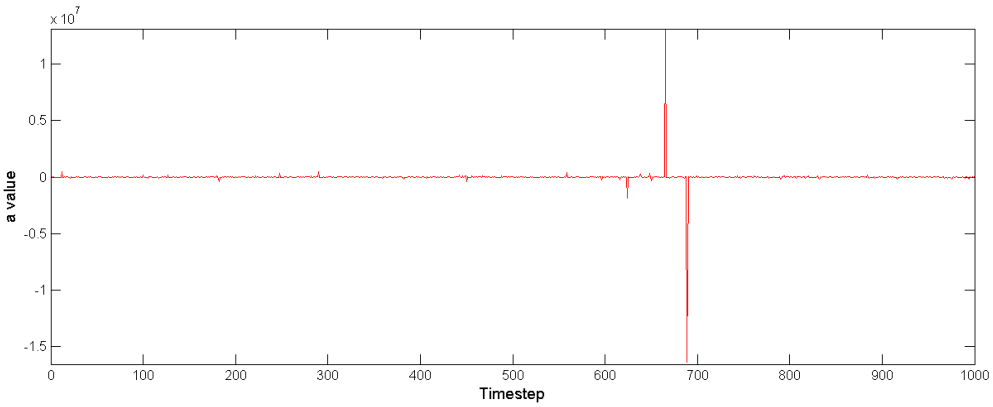

a

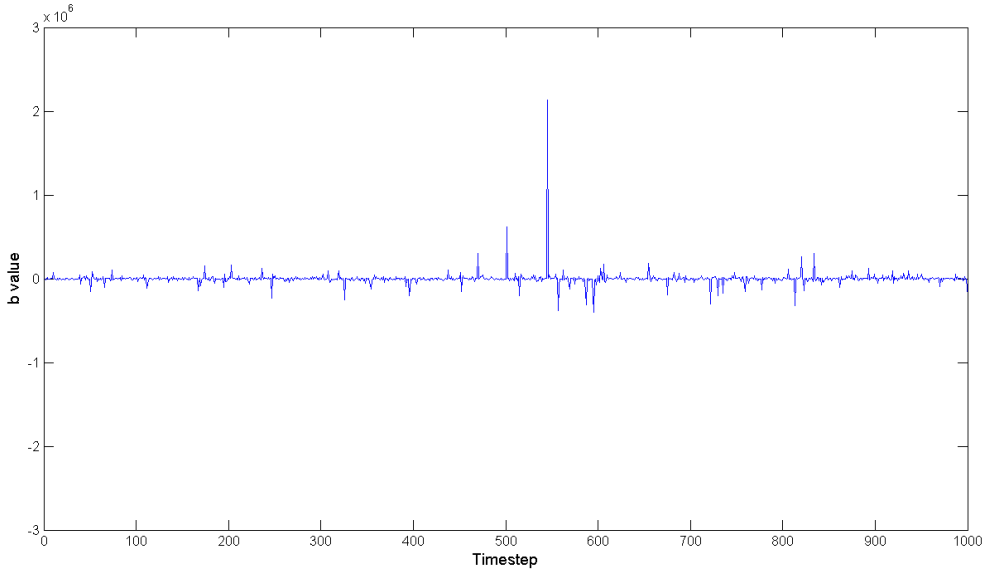

b

Figure 4.6 Values for a (a) and b (b) for 1000 timesteps for the initial condition of 1000 points uniformly distributed on the unit square.

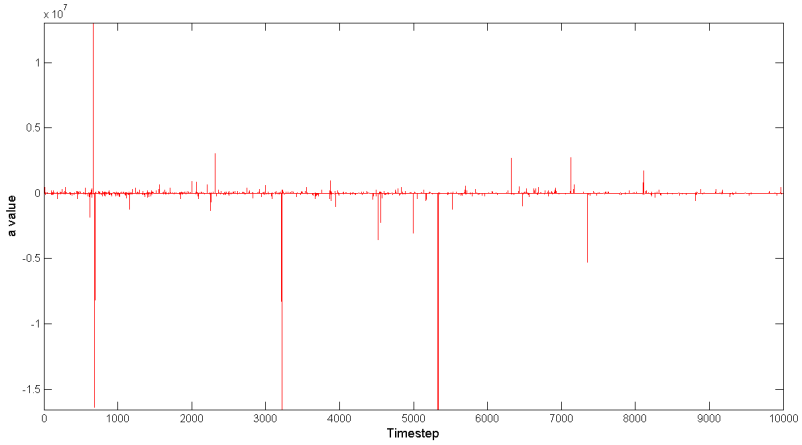

a

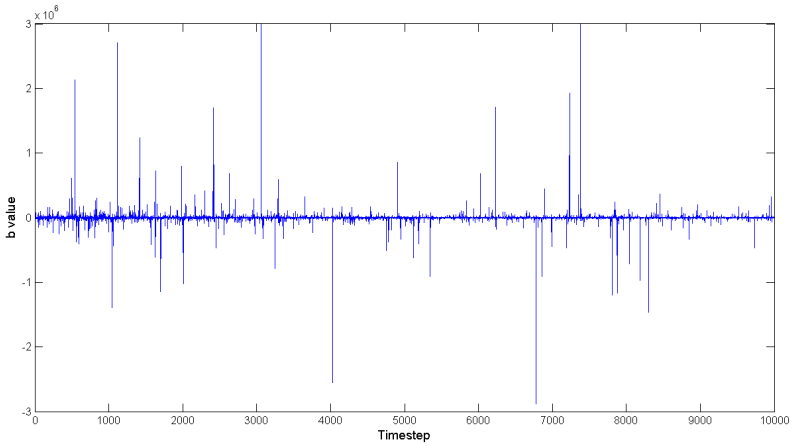

b

Figure 4.7 Values of a (a) and b (b) for 10000 timesteps for the initial condition of 1000 points uniformly distributed on the unit square. For both figures, large value spikes are reduced quickly within the next timestep. This behavior results from the corresponding swarm element being removed far from the axes by the control law.

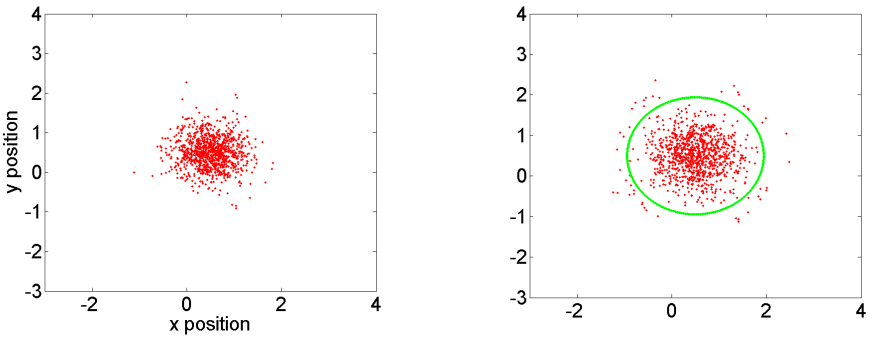

a. $n = 1000$ **b.** $n = 2000$

c. $n = 3000$ **d.** $n = 4000$

Figure 4.8 Progressive results for initial condition of 1000 points on a unit square. The green circle indicates the boundary between $QI \cup QIV$ and $QII \cup QIII$, which distinctly emerges after $n = 2000$. Elements outside of the boundary move away from the swarm center, whereas elements within the boundary are drawn towards the center of the swarm.

Chapter 5

Future Work

In Chapters 2 and 3 we have briefly described two methods for controlling swarms. The VARP method in Chapter 2 achieves global control by altering particle interaction laws, whereas the abstraction method in Chapter 3 sets controls of agents in a swarm by first defining its macroscopic characteristics.

Further direction for exploration could be to address the failures of the control method derived from the ψ function and more specifically determine how to correct these failures. The behavior seen with the "square" initial condition essentially arises from the boundary between the two groups of quadrants. A greater number of quadrants for 1000 points contained in the initial condition would, on average, assign a lesser number of elements per box, thereby making the discontinuities of the gradient of the magnitude of the coefficients $(f_j - N\pi_j)/(N\pi_j)$ of smaller magnitude. This might induce a less drastic shift in behavior from one radial region to the next.

On a more fundamental level, the way in which the χ^2 parameter is computed is another factor that drastically affects the observed behavior. The large values of the like of $1/(2x_i)$ are numerical artifacts that may not necessarily reflect the direction of the control law due to the finite nature of the implementation. The control method itself could be improved if the function for the parameter χ^2 has first-order derivatives.

Appendix A

Definitions

This section states the topology and differential geometry definitions that are used in this work. All definitions have been obtained from Isham (1989) and Isidori (1995).

Definition A.1 (Topology)**.** Let S be a set. A *topology* on S is a collection of subsets of S, called *open sets*, satisfying the axioms

i) The union of any number of open sets is open;

ii) The intersection of any finite number of open sets is open; and

iii) The set S and the empty set are open.

Definition A.2 (Topological space)**.** A set S with a topology is called a *topological space*.

Definition A.3 (Basis)**.** A *basis* of a topology on a set S is a collection of open sets, called *basic open sets* with the following properties

i) Elements of S are the unions of open basic sets;

ii) A nonempty intersection of two basic open sets is a union of open basic sets.

Definition A.4 (Homeomorphism)**.** Let S_1 and S_2 be topological spaces and let F be a map $F : S_1 \to S_2$. The map F is continuous if the inverse image of every open set in S_2 is an open set in S_1. The mapping F^{-1} is continuous if the image of every open set in S_1 is an open set in S_2. F is a *homeomorphism* if it is a continuous, open bijection.

Definition A.5 (Neighborhood)**.** A *neighborhood* of a point p in a topological space is any open set that contains that set.

Definition A.6 (Locally Euclidean space)**.** A *locally Euclidean space* X of dimension n is a topological space such that, for each $p \in X$, there exists a homeomorphism ϕ mapping some neighborhood of p onto a basic open set in $\mathbb{R}^n$.

Definition A.7 (Manifold)**.** A *manifold* N of dimension n is a topological space which is locally Euclidean of dimension n, has a countable basis, and any two different points p_1 and p_2 have disjoint neighborhoods.

Definition A.8 (Coordinate chart)**.** A *coordinate chart* of a point p in an n-dimensional manifold N is a pair (ϕ, U), where $U \subset N$ is a open set containing p and ϕ is a homeomorphism from U to $\mathbb{R}^n$.

Definition A.9 (Differentiable manifold)**.** A *differentiable manifold* M is a manifold with a differentiable structure defined in the following way: for M, there exists a collection of charts (ϕ_i, U_i), where $U_i \subset M$ and $\cup_{i=1} U_i = M$. Further, for every pair where $U_j \cap U_i \neq \emptyset$, $\phi_i \circ \phi_j^{-1}$ and $\phi_j \circ \phi_i^{-1}$ are both differentiable.

Definition A.10 (Parameterized curve)**.** A *parameterized curve* on a manifold M is a smooth; that is, C^∞, map σ from some open interval $(-\epsilon, \epsilon)$ of the real line to M.

Definition A.11 (Tangent)**.** Two curves σ_1 and σ_2 are *tangent* at a point p in M if

i) $\sigma_1(t) = \sigma_2(t) = p$; and

ii) In some local coordinate system $(x_1, \ldots, x^m)$ around the point the two curves are "tangent" in the usual sense as curves in $\mathbb{R}^m$.

Definition A.12 (Tangent vector)**.** A *tangent vector* at $p \in M$ is an equivalence class of curves in M where the equivalence relation is that two curves are tangent at the point p. We write the equivalence class of a particular curve σ as $[\sigma]$.

Definition A.13 (Tangent space)**.** The *tangent space* T_pM to M at the point p is the set of all tangent vectors at the point p.

Definition A.14 (Tangent bundle)**.** The *tangent bundle* TM is defined as $TM := \bigcup_{p \in M} T_pM$.

Definition A.15 (Differentiable map)**.** Let F be a mapping between two manifolds N and M. For each $n \in N$ and $m = F(n) \in M$, let the coordinate charts (ϕ, U) and (ψ, V) correspond to n and m respectively. If there exists a differentiable, bijective map between $\phi(U)$ and $\psi(V)$, then F is a *differentiable map* (between manifolds).

Definition A.16 (Differential)**.** Let $f : M \to N$ be a differentiable map between two manifolds M and N. The *differential* of f at point $p \in M$ is defined as the map

$$df_p : T_pM \to T_{f(p)}N$$

in the following way. For $v \in T_pM$ and $\lambda \in C^\infty(F(p))$,

$$(df_p(v))(\lambda) = v(\lambda \circ f).$$

Definition A.17 (Submersion)**.** Let $f : M \to N$ be a differentiable map between two manifolds N and M. The map f is a *submersion* at point $p \in M$ if df_p is a surjective linear map.

Definition A.18 (Real Lie group)**.** A *real Lie group* G is a set that

i) Has structure of a group, with an invertible operation and identity;

ii) Is a differentiable manifold with the properties that taking the product of two group elements, and taking the inverse of a group element, are smooth operations.

Bibliography

Barden, D., T. Karne, and H. Le. 1999. *Shape and Shape Theory*. New York: Wiley.

Belta, Calin A., and Vijay Kumar. 2004. Abstraction and control for groups of robots. *Robotics, IEEE Transactions on* 20(5):865–875.

Chuang, Y., M.R. D'Orsogna, D. Marthaler, A.L. Bertozzi, and L.S. Chayes. 2007. State transitions and the continuum limit for a 2D interacting, self-propelled particle system. *Physica D: Nonlinear Phenomena* 232(1):33–47.

D'Orsogna, M.R., Y.L. Chuang, A.L. Bertozzi, and L.S. Chayes. 2006. Self-propelled particles with soft-core interactions: Patterns, stability, and collapse. *Physical review letters* 96(10):104,302.

Isham, Chris J. 1989. *Modern Differential Geometry for Physicists*. Teaneck, NJ: World Scientific.

Isidori, Alberto. 1995. *Nonlinear Control Systems*. London, Great Britain: Springer, 3rd ed.

Kurabayashi, D., J. Ota, T. Arai, and E. Yoshida. 2002. Cooperative sweeping by multiple mobile robots. In *Robotics and Automation, 1996. Proceedings., 1996 IEEE International Conference on*, vol. 2, 1744–1749. IEEE.

Nguyen, B.Q., Y.L. Chuang, D. Tung, C. Hsieh, Z. Jin, L. Shi, D. Marthaler, A. Bertozzi, and R.M. Murray. 2005. Virtual attractive-repulsive potentials for cooperative control of second order dynamic vehicles on the Caltech MVWT. In *American Control Conference, 2005. Proceedings of the 2005*, 1084–1089. IEEE.

Small, C.G. 1996. *The Statistical Theory of Shape*. New York: Springer.